Bioorganic & Medicinal Chemistry 18 (2010) 6220–6229

Contents lists available at ScienceDirect

Bioorganic & Medicinal Chemistry

journal homepage: www.elsevier.com/locate/bmc

A class of novel carboline intercalators: Their synthesis, in vitro anti-proliferation, in vivo anti-tumor action, and 3D QSAR analysis

Jianhui Wu, Chunyu Li, Ming Zhao *, Wenjing Wang, Yuji Wang, Shiqi Peng *

College of Pharmaceutical Sciences, Capital Medical University, Beijing 100069, PR China

ARTICLE INFO

Article history:
Received 15 May 2010
Revised 16 July 2010
Accepted 17 July 2010
Available online 22 July 2010

Keywords:
Carboline
Anti-tumor activity
Intercalation
3D QSAR
Docking

ABSTRACT

Based on DOCK scores 18 *N*-(3-benzyloxycarbonylcarboline-1-yl)ethylamino acid benzylesters (**6a–r**) were synthesized as anti-tumor agents. Their IC_{50} values against five human carcinoma cell lines ranged from 11.1 μM to more than 100 μM. The in vivo assay identified five derivatives of them had no anti-tumor action, the anti-tumor activity of nine derivatives of them equaled that of cytarabine, and the anti-tumor activity of three derivatives of them was higher than that of cytarabine. The UV and fluorescence spectra, as well as the relative viscosity and melting temperature measurements of calf thymus DNA (CT DNA) with and without the representative compound suggested that DNA intercalation could be their action mechanism. The 3D QSAR analysis of *N*-(3-benzyloxycarbonylcarboline-1-yl)ethylamino acid benzylesters (**6a–r**) revealed that their in vivo anti-tumor activity significantly depends on the molecular electrostatic and steric fields of the side chain of the amino acid residue.

1. Introduction

DNA recognition is known to play a pivotal role in the anti-tumor efficacy of several anti-tumor agents, including groove binders, alkylating compounds and intercalating agents. DNA intercalation is known to play a pivotal role in the anti-tumor efficacy of several clinically used anti-tumor drugs including anthracyclines, acridines, and anthraquinones.[1] The discovery of new DNA intercalators has been a noticeable approach to push clinical therapy of cancer. Numerous intercalators have been reported recently,[2,3] and some β-carbolines, such as harmine and the derivatives, are involved.[4] The intercalation of β-carbolines towards DNA is correlated with cytotoxicity.[5,6] By intercalation β-carbolines inhibit topoisomerases I/II and finally damage DNA. As part of our ongoing efforts, we recently explored a series of β-carboline-3-carbonylamino acid benzylesters as potent anti-tumor derivatives of natural products. We demonstrated that the in vitro cytotoxicity of these benzylesters depended on their building blocks, that is, β-carboline-3-carboxylic acid, amino acid and benzyl moieties.[7] These requirements were successfully used for the design of *N*-(3-carboxyl-9-benzylcarboline-1-yl)ethylamino acids, and the in vitro anti-proliferation and the in vivo anti-tumor activities were analyzed with DOCK score.[8] In the present paper *N*-(3-carboxyl-9-benzylcarboline-1-yl)ethylamino acids were modified and a series of novel *N*-(3-benzyloxycarbonylcarboline-1-yl)ethylamino acid benzylesters were investigated.

2. Results and discussion

2.1. DOCK scores leading to *N*-(3-benzyloxycarbonylcarboline-1-yl)ethylamino acid benzylesters

DNA can be conveniently intercalated by planar heterocycles.[9–11] The LigandFit/LigandScore in DS Modeling 2.1 (Accelry Inc) and $d(CGATCG)_2$ oligonucleotide retrieved from the Protein Data Bank (1D12) has been widely used for the automated docking studies.[12,9,13] Firstly, the automated docking of *N*-(3-carboxyl-9-benzylcarboline-1-yl)ethylamino acids toward the cavity of $d(CGATCG)_2$ was carried out according to a general procedure, the DOCK scores were calculated and are listed in Table 1. Secondly, the possible derivatives of *N*-(3-carboxyl-9-benzylcarboline-1-yl)ethylamino acids were constructed by changing the position of the 9-benzyl. Finally, the automated docking of them toward the cavity of $d(CGATCG)_2$ was similarly carried out to calculate the DOCK scores. The DOCK scores of *N*-(3-carboxyl-9-benzylcarboline-1-yl)ethylamino acids and *N*-(3-benzyloxycarbonylcarboline-1-yl)ethylaminoacid benzylesters are listed in the left and right columns of Table 1, respectively. In the DOCK process it was observed that the binding cavity in the duplex was more suitable for benzylester derivatives than for 9-benzyl derivatives. In the DOCK process it was also observed that a graphic of benzylester derivative matching the binding cavity of $d(CGATCG)_2$ usually gained a high DOCK score. This ensured that the graphic could be

* Corresponding authors. Address: College of Pharmaceutical Sciences, Capital Medical University, Beijing 100069, PR China. Tel./fax: +86 10 8391 1528 (S.P.); tel./fax: +86 10 8280 2482 (M.Z.).
E-mail addresses: mingzhao@mail.bjmu.edu.cn (M. Zhao), sqpeng@mail.bjmu.edu.cn (S. Peng).

0968-0896/$ - see front matter Crown Copyright © 2010 Published by Elsevier Ltd. All rights reserved.
doi:10.1016/j.bmc.2010.07.043

Table 1
DOCK scores of carbolines with and without 9-benzyl

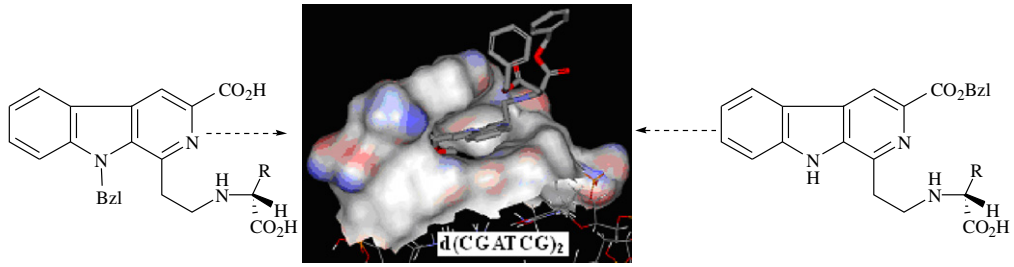

DOCK score	Compound/R	DOCK score
55.79	**6a**/H	74.21
51.12	**6b**/CH_3	72.46
49.14	**6c**/$CH(CH_3)_2$	65.97
46.26	**6d**/$CH_2CH(CH_3)_2$	61.84
46.71	**6e**/$CH(CH_3)CH_2CH_3$	52.71
52.83	**6f**/$CH_2CH_2SCH_3$	65.22
39.65	**6g**/$NH{=}NCH_2CH_2CH_2$	52.36
48.05	**6h**/$CH_2C_6H_5$	52.87
49.10	**6i**/indole-3-ylmethylene	62.19
59.91	**6j**/CH_2OH	67.37
50.81	**6k**/$CH(OH)CH_3$	60.50
40.68	**6l**/CH_2CONH_2	54.46
33.5	**6m**/$CH_2CH_2NH_2$	42.8
49.03	**6n**/$CH_2C_6H_4$-OH-p	68.41
60.73	**6o**/CH_2CO_2Bzl	85.38
30.26	**6p**/$CH_2(CH_2)_4NH_2$	43.17
52.77	**6q**/imidazole-3-ylmethylene	60.98
55.80	**6r**/$CH_2CH_2CO_2Bzl$	71.72

used as a model for the docking. The DOCK scores of *N*-(3-benzyloxycarbonylcarboline-1-yl)ethylamino acid benzylesters are significantly higher than those of *N*-(3-carboxyl-9-benzylcarboline-1-yl)ethylamino acids. This comparison suggests that *N*-(3-benzyloxycarbonylcarboline-1-yl)ethylamino acid benzylesters may comfortably adopt the cavity of $d(CGATCG)_2$ and high DOCK score benefits the in vitro anti-proliferative and in vivo anti-tumor activities. As seen in Table 2, the IC_{50} of *N*-(3-benzyloxycarbonylcarboline-1-yl)ethylamino acid benzylesters against $HepG_2$ and Hela cells range from 13.5 μM to more than 100 μM, while the IC_{50} of *N*-(3-carboxyl-9-benzylcarboline-1-yl)ethylamino acids against $HepG_2$ and Hela cells range from 26.5 μM to more than 400 μM. Besides, on S180 mouse model the effective dose of *N*-(3-benzyloxycarbonylcarboline-1-yl)ethylamino acid benzylesters is 10-fold lower than that of *N*-(3-carboxyl-9-benzylcarboline-1-yl)ethylamino acids.[8]

Table 2
IC_{50} of **6a–r** against $HepG_2$, Hela, Bel7402, K562, and B16 cells[a]

Compd	$HepG_2$	Hela	Bel7402	K562	B16
Ara-C	0.2 ± 0.1	—	34.2 ± 2.1	33.5 ± 1.8	—
6a	50.0 ± 8.3	26.8 ± 4.2	53.2 ± 7.6	47.1 ± 6.2	75.4 ± 9.1
6b	>100	76.4 ± 1.2	100 ± 5.2	48.2 ± 8.4	20.5 ± 2.3
6c	29.2 ± 1.2	25.5 ± 2.2	20.3 ± 3.1	20.9 ± 1.8	28.8 ± 1.3
6d	25.2 ± 2.1	22.5 ± 3.1	43.5 ± 1.4	21.5 ± 1.8	50.2 ± 3.2
6e	>100	>100	>100	>100	19.2 ± 2.1
6f	18.7 ± 1.2	28.8 ± 1.5	25.8 ± 2.1	13.5 ± 1.0	61.1 ± 2.8
6g	17.1 ± 1.2	25.8 ± 1.5	52.8 ± 2.2	20.1 ± 1.9	71.8 ± 2.2
6h	>100	>100	>100	>100	28.1 ± 2.1
6i	60.0 ± 3.2	59.5 ± 2.7	39.0 ± 2.1	14.9 ± 1.2	20.7 ± 1.3
6j	19.9 ± 1.1	20.3 ± 2.0	54.6 ± 6.8	19.7 ± 2.1	60.3 ± 8.4
6k	26.0 ± 2.1	15.2 ± 1.2	>100	38.3 ± 3.2	38.4 ± 3.3
6l	>100	97.2 ± 15.2	>100	63.6 ± 10.3	17.1 ± 4.5
6m	35.9 ± 5.2	71.0 ± 8.2	81.3 ± 6.7	>100	42.5 ± 6.2
6n	>100	16.7 ± 2.0	23.7 ± 2.3	18.9 ± 1.9	24.5 ± 2.8
6o	>100	>100	60.3 ±	>100	11.1 ± 4.5
6p	36.3 ± 4.2	33.9 ± 4.8	14.9 ± 3.2	15.4 ± 2.8	49.4 ± 5.4
6q	>100	63.6 ± 7.2	36.9 ± 5.3	14.4 ± 3.1	60.0 ± 4.6
6r	63.1 ± 10.2	54.9 ± 8.2	>100	18.5 ± 4.5	66.4 ± 5.2

[a] Ara-C = cytarabine, $n = 6$, IC_{50} is represented by mean ± SD μM.

2.2. Synthesis of *N*-(3-benzyloxycarbonylcarboline-1-yl)-ethylamino acid benzylesters

N-(3-Benzyloxycarbonylcarboline-1-yl)ethylamino acid benzylesters (**6a–r**) were synthesized according to the seven-step-route depicted in Scheme 1. Using a common procedure, L-Trp was converted to L-Trp-OMe (92% yield). The Pictet-Spengler condensation of L-Trp-OMe and 1,1,3,3-tetramethoxypropane provided methyl 1-(2,2-dimethoxyethyl)-1,2,3,4-tetrahydro-β-carboline-3-carboxylate (**1**) in 89% yield. In the presence of $KMnO_4$ the piperidine ring of **1** was aromatized to form β-carboline-3-carboxylic acid methylester (**2**) in 80% yield. At 0 °C **2** was treated with 2 N aqueous of NaOH to saponify and form **3**. Esterification of **3** and benzyl bromide provided benzyl 1-(2,2-dimethoxyethyl)-β-carboline-3-carboxylate (**4**) in 74% yield. In the presence of HOAc and HCl the acetal **4** was hydrolyzed to aldehyde **5** in 67% yield. Reduced amination of **5** and amino acid banzylesters provided *N*-(3-benzyloxycarbonyl-9-*H*-carboline-1-yl)ethylamino acid benzylesters (**6a–r**) in 35–88% yields.

2.3. IC_{50} of 6a–r against the proliferation of carcinoma cells

To predict the tumoricidal indication of **6a–r** in the in vitro anti-proliferation assays five carcinoma cell lines, $HepG_2$ (human

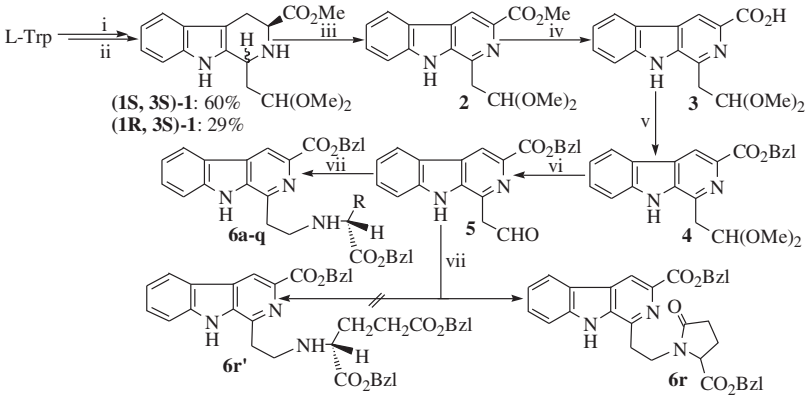

Scheme 1. Synthesis of *N*-(3-benzyloxycarbonyl-9-*H*-carboline-1-yl)ethylamino acid benzylesters **6a**–**r**. Reagents and conditions: (i) $SOCl_2$, MeOH; (ii) HCl, 1,1,3,3-tetramethoxypropane, MeOH; (iii) $KMnO_4$, DMF; (iv) NaOH, H_2O, MeOH; (v) K_2CO_3, $BrCH_2C_6H_5$, DMF/THF; (vi) HCl, HOAc, H_2O; (vii) NaOH, $NaBH_3CN$ and amino acid benzylester; **6a** R = H, **6b** R = CH_3, **6c** R = $CH(CH_3)_2$, **6d** R = $CH_2CH(CH_3)_2$, **6e** R = $CH(CH_3)CH_2CH_3$, **6f** R = $CH_2CH_2SCH_3$, **6g** R = NH = $NCH_2CH_2CH_2$, **6h** R = $CH_2C_6H_5$, **6i** R = indole-3-ylmethylene, **6j** R = CH_2OH, **6k** R = $CH(OH)CH_3$, **6l** R = CH_2CONH_2, **6m** R = $CH_2CH_2CONH_2$, **6n** R = $CH_2C_6H_4$–OH-*p*, **6o** R = CH_2CO_2Bzl, **6p** R = $CH_2(CH_2)_4NH_2$, **6q** R = imidazole-3-ylmethylene, **6r** R = $CH_2CH_2CO_2Bzl$.

hepatocellular liver carcinoma cell line), Hela (human epithelial cervical cancer), Bel7402 (human hepatoma cell line), K562 (human immortalized myelogenous leukemia line) and B16 (mouse melanoma cell line), were used. In the assays the cells were exposed to serial concentrations (0.1–200 μM) of **6a–r** or cytarabine (positive control), and the standard MTT assays were performed. The IC_{50} values are summarized in Table 2. The data indicate that **6a–r** efficiently inhibit the proliferation of these cells. The IC_{50} values range from 11.1 μM to more than 100 μM with **6c** as the most potent compound. It was explored that the cells show different sensitivity to **6a–r**. HepG2 cells were more sensitive to **6c,d,f,g,j,k** than to the others, B16 cells was sensitive to **6o** only, Hela cells was sensitive to **6n** only, while no cells were practically sensitive to **6e** and **6h**. Due **6a–r** having common β-carboline ring a preliminary structure–activity relationship was analyzed by correlating their individual amino acid side chain with the corresponding in vitro activity. It was the case that the compounds, such as **6c,d,f,g,j,k**, with flexible side chain usually gave low IC_{50} value.

Table 3
Effects of **6a**–**r** on tumor weights of S180 mice[a]

Compd	Tumor weight	%Inhibition
NS	1.62 ± 0.28	
Ara-C	1.22 ± 0.17[b]	24.3 ± 0.5
6a	1.56 ± 0.27	3.5 ± 0.4
6b	1.26 ± 0.19[b]	22.0 ± 0.5
6c	1.07 ± 0.59[b]	34.0 ± 0.8
6d	0.80 ± 0.23[d]	50.9 ± 0.7
6e	1.09 ± 0.17[b]	33.9 ± 0.6
6f	1.37 ± 0.30[c]	15.3 ± 1.1
6g	1.50 ± 0.41	7.1 ± 1.8
6h	1.51 ± 0.31	6.6 ± 0.6
6i	1.27 ± 0.31[c]	22.2 ± 0.6
6j	1.02 ± 0.09[d]	36.7 ± 0.6
6k	1.05 ± 0.42[b]	34.8 ± 0.7
6l	1.39 ± 0.33	14.0 ± 0.9
6m	1.70 ± 0.55	−5.3 ± 0.9
6n	1.10 ± 0.24[b]	31.7 ± 0.5
6o	0.71 ± 0.18[d]	56.1 ± 0.7
6p	1.15 ± 0.32[b]	28.9 ± 1.3
6q	1.04 ± 0.32[b]	35.4 ± 0.5
6r	1.14 ± 0.25[b]	29.4 ± 0.4

[a] Ara-C = cytarabine, NS = normal saline, $n = 12$, dose of Ara-C and **6a–r**: 8.9 μmol/kg, tumor weight is represented by $\bar{x} \pm$ SD g.
[b] Compared to NS $p < 0.01$.
[c] Compared to NS $p < 0.05$.
[d] Compared to NS and Ara-C $p < 0.01$.

2.4. Effect of 6a–r on the tumor weight of S180 mice

In the previous paper it was observed that due to the in vivo stability of the β-carboline ring of 9-benzyl derivatives their in vitro activities did not quite correlate with their in vivo activities.[8] To continue this observation in the present in vivo evaluation all compounds were assayed. In the assays the tumor weight of **6a–r** treated S180 mice was recorded. As shown in Table 3, when the mice were given a daily ip injection of 8.9 μmol/kg of **6a–r** in 0.2 ml of normal saline (NS) for seven consecutive days, the tumor weights ranged from 0.71 g to 1.70 g (NS receiving mice, 1.62 g), and 13 derivatives of **6a–r** significantly decreased the tumor weight of the treated mice. The efficacy of **6d,j,o** (tumor weight ranging from 0.71 g to 1.02 g), the most potent compounds for these five carcinoma cells, is significantly higher than that of cytarabine (positive control, tumor weight 1.22 g) and the efficacy of **6b,c,e,k,n,p–r** (tumor weight ranging from 1.05 g to 1.26 g) essentially equals that of cytarabine. The different anti-tumor efficacy and different amino acid residue of **6a–r** suggest that the anti-tumor activity correlates with the side chain of the amino acid residue. On the other hand, the comparison of the data of Table 2 and Table 3 suggests that similarly to 9-benzyl derivatives for the present benzylesters the in vitro activities also does not quite correlate with the in vivo activities.

Table 4
Effect of the dose of **6o** and **6q** on the tumor weight of S180 mice[a]

Compd	Dose (μmol/kg)	Tumor weight	%Inhibition
Ara-C	89.0	0.73 ± 0.20[b]	54.8 ± 14.5
	8.9	1.22 ± 0.17[c]	24.3 ± 0.5
	0.89	1.52 ± 0.30	6.8 ± 0.7
6o	89.0	0.43 ± 0.11[b]	73.5 ± 4.0
	8.9	0.71 ± 0.18[c]	56.1 ± 0.7
	0.89	0.96 ± 0.31	40.6 ± 3.6
6q	89.0	0.63 ± 0.27[b]	60.7 ± 14.3
	8.9	1.04 ± 0.32[c]	35.4 ± 0.5
	0.89	1.54 ± 0.39	6.3 ± 1.2

[a] Ara-C = cytarabine, $n = 12$, tumor weight is expressed by $\bar{x} \pm$ SD g.
[b] Compared to 8.9 μmol/kg of **6o** and **6q** $p < 0.01$.
[c] For Ara-C and **6q**: compared to 0.89 μmol/kg of **6q** $p < 0.01$, for **6o**: compared to 0.89 μmol/kg of **6o** $p < 0.05$.

2.5. Dose-dependent in vivo anti-tumor activity of 6o,q

Two representatives (**6o** and **6q**) were selected to examine the dose-dependent action. The tumor inhibition of 89.0, 8.9, and 0.89 μmol/kg of **6o** and **6q** is 73.5%, 56.1%, and 40.6% as well as 60.7%, 35.4%, and 6.3%, respectively (Table 4). Therefore, **6o** and **6q** dose-dependently inhibit the growth of the tumor. The minimal effective dose of **6o** and **6q** is 0.89 μmol/kg and 8.9 μmol/kg, respectively.

2.6. Action mechanism of 6a–r

Small molecule-induced variation of DNA spectra has been widely used to identify the intercalation.[14–17] To examine DNA intercalation of **6a–r**, calf thymus DNA (CT DNA) was selected as the model DNA, **6d**, one of the most potent compounds that their in vitro activities substantially correlate with their in vivo activities, was selected as model compound. The UV, fluorescence spectra, viscosity, and melting temperature of CT DNA alone and CT DNA plus **6d** were compared. These comparisons provided spectral evidence for DNA intercalation of **6d**.

2.6.1. UV spectra of CT DNA without and with 6d

In the UV experiments the spectra (Fig. 1) of a solution of CT DNA in PBS (final concentration 240 μM) and the spectra of the solution of CT DNA (final concentration 240 μM) plus **6d** (final concentration 27, 54, 81, 108 μM) in PBS were determined on a Shimadzu 2550 spectrophotometer over 220–400 nm. Figure 1 explores that **6d** induces a hypochromic effect (53.04%) and hypsochromic shift (2.5 nm).

2.6.2. Fluorescence spectra of CT DNA without and with 6d

In the fluorescence experiments the spectra (Fig. 2) of CT DNA and CT DNA plus **6d** were determined at 300 K using of fluorescence spectroscopy. The solution of **6d** in PBS (0.5 μM) was titrated with 10 μl of the solution of a series concentration (0, 8, 16, 24, 32, 40, 48, 56, 64, and 72 μM) of CT DNA in PBS. A series of variations of the fluorescence intensity of **6d** were recorded on a Shimadzu RF-5310PC spectrofluorometer at 382 nm of emission wavelength (the excitation wavelength is 254 nm). The fluorescence quenching phenomenon, that is, CT DNA induced concentration-dependent decrease of fluorescence intensity of **6d**. When the concentration of CT DNA is 72 μM **6d** gains the minimal fluorescence intensity (34.65% of decrease). These suggest **6d** having a DNA intercalation mechanism.

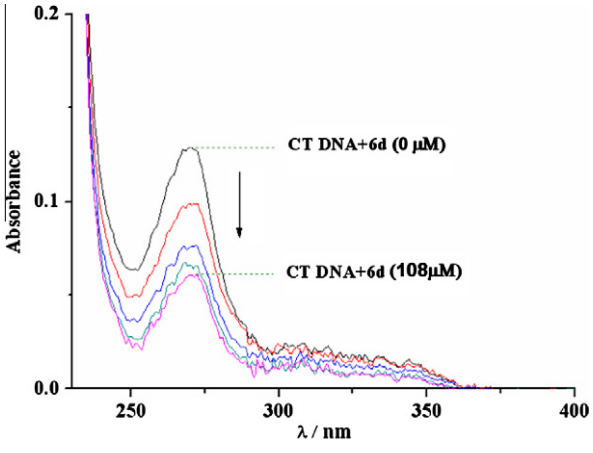

Figure 1. Hypochromic effect and hypsochromic shift occurred in the UV spectra of CT DNA (final concentration 240 μM) plus **6d** (final concentration 0, 27, 54, 81, 108 μM) in PBS.

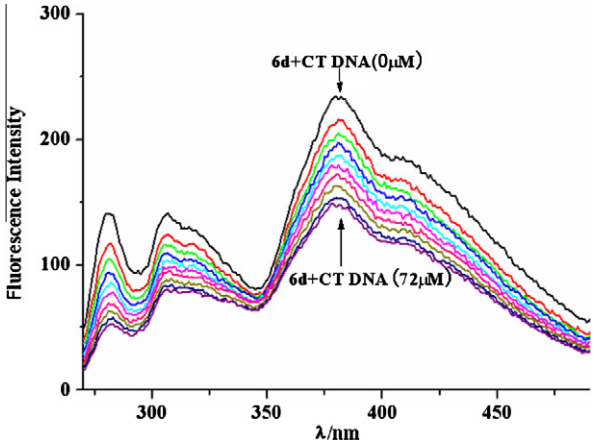

Figure 2. Fluorescence spectra of **6d** in PBS (concentration 0.5 μM, λ_{em} = 382 nm, λ_{ex} = 254 nm) explain the fluorescence quenching induced by 10 μl of the solution of CT DNA in PBS (8, 16, 24, 32, 40, 48, 56, 64, 72 μM).

2.6.3. Viscosity of CT DNA without and with 6d[18,19]

In DNA intercalation to accommodate and bind small molecule DNA base pairs are pushed apart and consequently lead to viscosity increase. Thus viscosity increase is widely used to define the intercalation. Here the relative viscosity of the sample solutions of [**6d**]/[CT DNA] in the ratios of 0–0.36 were measured. Figure 3 indicates that **6d** concentration-dependently increases the relative viscosity of CT DNA. This could be considered as the result of DNA intercalation of **6d**.

2.6.4. Melting temperature of CT DNA without and with 6d[20,21]

The thermal melting of DNA is widely used to measure the thermostability of DNA double helix. Once the temperature of DNA solution is high enough the double strands dissociate to single stand, and the temperature that induces the absorbance to increase 50% is termed as melting temperature (T_m). The temperature of the solution of CT DNA in PBS (100 μM) and the solution of CT DNA (100 μM) plus **6d** (18 μM) in PBS rose at a rate of 1 °C/min and the absorbance was monitored at 260 nm. The melting curves of CT DNA and CT DNA plus **6d** are shown with Figure 4. The biphasic melting curve of CT DNA plus **6d** is similar to that of CT DNA plus daunomycin.[22] The T_m of CT DNA plus **6d** in PBS is 13.8 ± 0.5 °C higher than that of CT DNA alone indicates that in the presence of **6d** the double strands of CT DNA are stabilized. This additional stability should be attributed to DNA intercalation of **6d**.

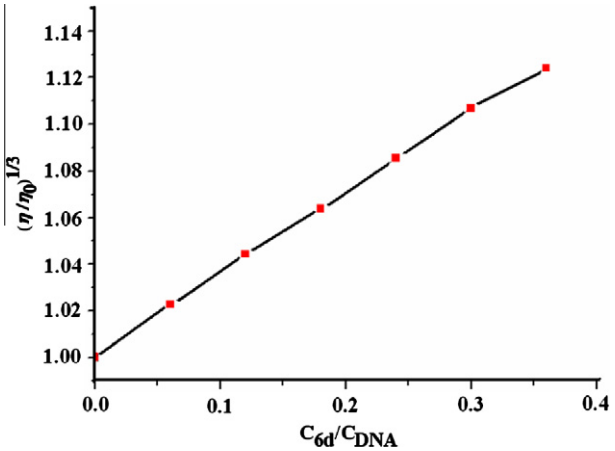

Figure 3. Effect of **6d** on the relative viscosity of CT DNA (300 μM).

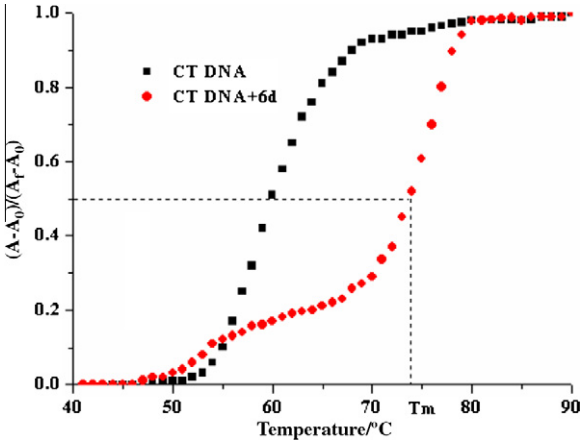

Figure 4. Thermal denaturation curves of CT DNA with and without **6d**. T_m measurements were performed in PBS at pH 7.4 with a **6d**/DNA ratio of 0.18.

2.6.5. 3D QSAR analysis of 6a–r

To elucidate the effects of the side chain of amino acid on the anti-tumor activity of **6a–r**, the activity is expressed with the tumor inhibition rate. For 3D QSAR the training set (**6a–f,h,j,l–r**) and the test set (**6g,i,k**) selections done manually such that they populate the wide range of anti-tumor activity in a similar proportions.

The 3D QSAR module of Cerius2 was followed to quantitatively correlate the tumor inhibition rate with the structure of **6a–f,h,j,l–r**. To establish valid 3D QSAR models a proper alignment procedure of **6a–r** was performed using the target model align strategy in the align module within Cerius2. With an assumption that each structure of **6a–r** binds the same site of the receptor and exhibits activity, they were aligned in a pharmacological active orientation. To obtain a consistent alignment the common moiety carboline-3-carboxylic acid benzyl ester was selected as the template for superposing **6a–r**. The method used for performing the alignment was the maximum common subgraph (MCS).[23] MCS looks at molecules as points and lines, and uses the techniques out of graph theory to identify the patterns. Then MCS finds the largest subset of atoms in carboline-3-carboxylic acid benzyl ester that shared by **6a–f,h,j,l–r**. This subset was used for the alignment. A rigid fit of atom pairings was performed to superimpose each structure onto the target model carboline-3-carboxylic acid benzyl ester. The stereoview of aligned **6a–r** is shown in Figure 5. The alignment stereoview explores that to superimpose onto carboline-3-carboxylic acid benzyl ester the 1-ethylamino acid residue of each structure has to take individual conformation. The individual conformation will influence the anti-tumor activity.

Molecular field analysis (MFA) was performed for **6a–r** by using the QSAR module of Cerius2.[24] A five-step-procedure consisted of generating conformers, energy minimization, matching atoms and aligning molecules, setting preferences, and regression analysis was automatically practiced in MFA. Molecular electrostatic and steric fields were created by use of proton, hydroxyl group and methyl group as the probe, respectively. These fields were sampled at each point of a regularly spaced grid of 1 Å. An energy cutoff of ±30.0 kcal/mol was set for both electrostatic and steric fields. The totally generated grid points were 672. Though the spatial and structural descriptors such as dipole moment, polarizability, radius of gyration, number of rotatable bonds, molecular volume, principal moment of inertia, *A* log *P*98 (the calculated logarithm of partition coefficient from the implementation of the atom-type-based method using the latest published set of parameters), number of hydrogen bond donors and acceptors, and molar refractivity were also considered, only the highest variance holder proton, methyl, and hydroxyl descriptors were used. Regression analysis was carried out using the genetic partial least squares (G/PLS) method consisting of 50,000 generations with a population size of 100. The number of components was set to 5. Cross-validation was performed with the leave-one-out procedure. PLS analysis was scaled, with all variables normalized to a variance of 1.0.

The regions where variations in the steric or electrostatic features of **6a–r** in the training set lead to increase or decrease the activity were specified. Proton descriptor with positive coefficient indicates a region favorable for electropositive group, while negative coefficient indicates electronegative group required at this position. Methyl descriptor with positive coefficient indicates a region favorable for large group, while negative coefficient indicates small group required at this position. Hydroxyl descriptor with positive coefficient indicates a region favorable for hydrogen bond forming group, while negative coefficient indicates hydrogen bond forming group not required at this position. The MFA model for the activity of **6a–r** in terms of the most relevant descriptors proton, hydroxyl group and methyl group is expressed by Eq. 1.

$$\begin{aligned}\%\text{Inhibition} = {} & 2.45475 + 0.498953(H^+/441) \\ & - 0.729572(H^+/357) + 1.90153(CH_3/404) \\ & - 0.364508(HO^-/693) + 1.30811(HO^-/694) \end{aligned} \quad (1)$$

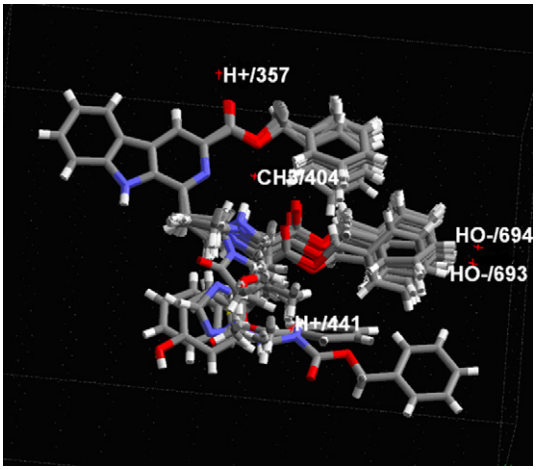

Figure 5. Alignment stereoview of **6a–r** used for molecular field generation.

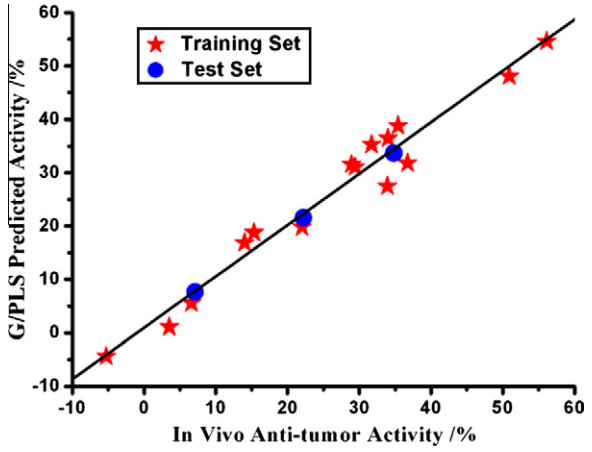

Figure 6. Graph of the tested in vivo anti-tumor activities against calculated in vivo anti-tumor activities.

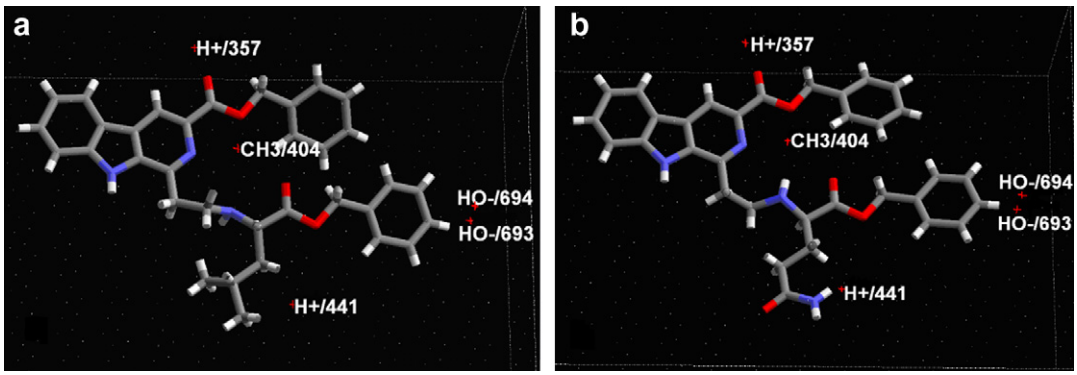

Figure 7. Electrostatic environment of **6d** (a) with high in vivo anti-tumor activity and **6m** (b) with low in vivo anti-tumor activities within the grid with 3D points of Eq. 1.

The data points (n), correlation coefficient (r) and square correlation coefficient (r^2) of Eq. 1 were 15, 0.981, and 0.963, respectively. The correlation of the tested anti-tumor activities on S180 mouse model with the calculated anti-tumor activities from Eq. 1 is explained with Figure 6.

In Eq. 1 one term of H^+/441 with positive coefficient from proton descriptor, which means that at this position electron-releasing group will decrease the in vivo anti-tumor activity, one term of H^+/357 with negative coefficients from proton descriptor, which means that at this position electron-releasing group will increase the in vivo anti-tumor activity, one term of CH_3/404 with positive coefficient from methyl descriptor, which means that at this positions large group will decrease the in vivo anti-tumor activity, and one term of HO^-/694 with positive coefficient from hydroxyl descriptor, which means that at this position hydrogen bond forming group will increase the activity, and one term of HO^-/693 with negative coefficients from hydroxyl descriptor, which means that at this position hydrogen bond forming group will decrease the activity, are involved.

As the examples Figure 7 gives the electrostatic and environments of one representative **6d** with high in vivo anti-tumor activity, and **6m** with low in vivo anti-tumor activity within the grid with 3D points of Eq. 1. Besides the same electrostatic and environments as carboline-3-carboxylic acid benzyl ester moiety **6d** has electron-releasing group near H^+/441 thus resulting in increasing the in vivo anti-tumor activity. Besides the same electrostatic and environments as carboline-3-carboxylic acid moiety **6m** has electron-withdrawing group near H^+/441 thus resulting in decreasing the in vivo anti-tumor activity.

Predict power of Eq. 1 was demonstrated by comparing the calculated and the tested in vivo anti-tumor activities of the test set (Table 5 **6g,i,k**). The results indicate that Eq. 1 rationally gives in vivo anti-tumor activities for the test set and the errors range from +0.5% to −1.1%. The calculated activity is approximate to the experimental activity means that Eq. 1 is practical to accurately predict the anti-tumor activity of the derivatives of carboline-3-carboxylic acid benzyl ester.

Table 5
Predict and test anti-tumor activities of **6g**,**i**,**k**

Compd	Tumor inhibition (%)		
	Predict value	Test value	Error
6g	7.6	7.1	+0.5
6i	21.6	22.2	−0.6
6k	33.7	34.8	−1.1

3. Conclusion

N-(3-Benzyloxycarbonyl-9-*H*-carboline-1-yl)ethylamino acid benzylesters **6a–r** could be prepared in desirable yields by using a seven-step route. The in vitro anti-proliferation assays of **6a–r** with five human carcinoma cell lines identified K562 cells to be more sensitive than the others. The in vivo anti-tumor activity assays of **6a–r** identified **6d** and **6o** having the highest efficacy. The tumor weight of 8.9 μmol/kg of **6d** (0.80 ± 0.23 g) or **6o** (0.71 ± 0.18 g) treated mice closes that (0.73 ± 0.20 g, p >0.05) of 89 μmol/kg of cytarabine treated mice. The UV and fluorescence spectra, as well as the relative viscosity and melting temperature measurements of CT DNA with or without **6d** suggest **6a–r** been capable of intercalating toward DNA. The 3D QSAR studies were carried out by building MFA models for the building of a strategy and consequently for the improvement of the activity of the compounds. The 3D QSAR analysis of **6a–r** reveals that the in vivo anti-tumor activity depends on the molecular electrostatic and steric fields of the side chains of the amino acid moieties. In general, electron-drawing group at 441 position, electron-releasing group at 357 position, small group at 404 position group and hydrogen bond forming group at 694 position and hydrophobic group at 693 position are necessary for higher anti-tumor. The DOCK study revealed that these ligands bind in the base pairs of d(CGATCG)2. The comfort of the β-carboline ring in the binding cavity in the duplex is crucial for the in vivo anti-tumor activity. The results of the in vivo evaluation rationally correlated with the results of the 3D QSAR and with the results of the DOCK, for instance the experimental tumor inhibition of **6d**/**6m** (50.9%/−5.3%) rationally correlated with their calculated tumor inhibition (51.4%/−5.8%) and with their DOCK score (61.84/42.8).

4. Experimental

4.1. General

All chemicals were purchased from commercial suppliers and were purified when necessary. Protected amino acids with L-configuration were purchased from Sigma Chemical Co. Chromatography was performed on Qingdao Silica Gel H. The purities of the intermediates and the products were measured by TLC analysis (Merck silica gel plates of type 60 F_{254}, 0.25 mm layer thickness) and HPLC analysis (waters, C_{18} column, 4.6 × 150 mm). Melting points were determined in capillary tubes on an electrothermal SM/XMP apparatus and without correction. UV spectra were measured on Shimadzu UV 2550. ESI-MS was determined by Micromass Quattro micro TM API, Waters Co. ^{1}H NMR (500 Hz) and ^{13}C NMR (125 Hz) spectra were acquired on a Bruker AC 300 spec-

trometer in $CDCl_3$ or in DMSO-d_6 with TMS as internal standard, and chemical shifts are expressed in ppm. Optical rotations were determined with a Jasco P-1020 Polarimeter. Statistical analysis of all the biological data was carried out by use of ANOVA test, $p < 0.05$ is considered significant.

4.2. General procedure for preparing amino acid benzylesters hydrochloride

At room temperature 0.02 mol amino acid was added to the solution of 10.0 g polyphosphoric acid and 50 ml of benzyl alcohol. The reaction mixture was stirred at 90 °C for 8 h. TLC indicated complete disappearance of amino acid. The reaction mixture was cooled to room temperature, mixed with the solution of 20 ml of concentrated sulfuric acid in 200 ml of water, treated with 20 ml of ether, the aqueous phase was separated and neutralized with aqueous solution of sodium carbonate adjusted to pH 10. The solution was extracted with ether (370 ml) and the ether phase was dried with anhydride magnesium sulfate. After filtration the filtrate was bubbled with hydrogen chloride to precipitate the hydrochloride of amino acid benzyl ester as colorless powder.

4.3. Methyl 1-(2,2-dimethoxyethyl)-1,2,3,4-tetrahydro-β-carboline-3-carboxylate (1)

A suspension of 5.0 g (24.5 mmol) of L-tryptophan methylester, 50 ml of MeOH and 6.0 ml (23.6 mmol) of 1,1,3,3-tetramethoxypropane was adjusted pH 1–2 with HCl (5 N) and stirred at 45 °C for 48 h. After cooling the solvent was evaporated under vacuum, the residue was diluted with water and the aqueous solution was extracted with EtOAc (30 ml × 3). The organic phase was separated, washed successively with 10% sodium carbonate and saturated NaCl, dried over anhydrous sodium sulfate, filtered and the filtrate was evaporated under vacuum. The residue was purified by silica gel chromatography ($CHCl_3$/MeOH, 30:1) to provide 1.57 g (29%) of **(1*S*,3*S*)-1** and 3.24 g (60%) of **(1*R*,3*S*)-1** as pale yellow oil. FAB-MS (m/e) 319 $[M+H]^+$.

4.4. Methyl 1-(2,2-dimethoxyethyl)-β-carboline-3-carboxylate (2)

A mixture of 4.3 g (13.5 mmol) of **1** and 100 ml of DMF was stirred at 0 °C until a clear solution was formed, to which 3.04 g (19.3 mmol) of $KMnO_4$ was then added. The reaction mixture was stirred at 0 °C for 1 h, and then at room temperature for 3 h until TLC ($CHCl_3$/MeOH, 15:1) indicated the complete disappearance of starting material. The formed precipitate was filtered and the filtrate was evaporated under vacuum. The residue was diluted with 100 ml of EtOAc and the solution was washed successively with water and saturated aqueous of NaCl. The organic phase was separated and dried over anhydrous sodium sulfate. After filtration the filtrate was evaporated under vacuum. The residue was solidified in acetone to give 3.47 g (80.3%) of the title compound as a yellow power. Mp 135–136 °C, ESI/MS (m/e) 315 $[M+H]^+$, ^{1}H NMR ($CDCl_3$) δ: 9.63 (1H, s), 8.81 (1H, s), 8.16 (1H, d, J = 8.0 Hz) 7.54–7.56 (4H, m), 7.30–7.42 (4H, m), 5.53 (2H, s), 4.82 (1H, s), 3.58 (2H, d, J = 4.0 Hz), 3.41 (6H, s); ^{13}C NMR ($CDCl_3$) δ: 166.04, 141.36, 140.74, 137.50, 137.17, 136.31, 128.64, 128.51, 128.45, 128.18, 122.09, 121.89, 120.73, 117.07, 112.12, 105.47, 67.02, 54.79, 40.89. Anal. Calcd for $C_{17}H_{18}N_2O_4$: C, 64.96; H, 5.77; N, 8.91. Found: C, 64.74; H, 5.89; N, 8.70.

4.5. 1-(2,2-Dimethoxyethyl)-β-carboline-3-carboxylic acid (3)

At 0 °C to the solution of 499 mg (1.59 mmol) of **2** in 7 ml of methanol was adjusted to pH 11 with 2 N aqueous of NaOH. The reaction mixture was stirred at 0 °C for 3.5 h and TLC ($CHCl_3$/CH_3OH, 10:1) indicated the complete disappearance of **2**. The reaction mixture was adjusted to pH 7 with aqueous solution of $KHSO_4$. The solution was evaporated under vacuum to remove methanol, adjusted pH 2 with aqueous solution of $KHSO_4$ and extracted with EtOAc (30 ml × 3). The combined EtOAc was successively washed with saturated aqueous solution of NaCl (20 ml × 3) and dried with anhydrous Na_2SO_4, filtered and concentrated in vacuum to give the title compound as pale yellow oil. The oil was used for the next step without any further purification.

4.6. Benzyl 1-(2,2-dimethoxyethyl)-β-carboline-3-carboxylate (4)

A mixture of 477 mg (1.59 mmol) of **3**, 10 ml of anhydrous DMF and 329 mg (2.39 mmol) of K_2CO_3 was stirred at room temperature for 2 h. To this mixture 297 mg (1.74 mmol) of benzyl bromide was added and the reaction mixture was stirred for 21 h. To this mixture 200 g of ice was added and the solution was extracted with EtOAc (20 ml × 3). The organic phase was separated, washed with saturated aqueous NaCl and dried over anhydrous sodium sulfate. After filtration the filtrate was evaporated under vacuum. The residue was purified with silica gel chromatography (petroleum ether/EtOAc, 2:1) to give 473 mg (74%) of the title compound as colorless powder. ESI/MS (m/e) 391 $[M+H]^+$; ^{1}H NMR ($CDCl_3$) δ: 9.68 (1H, s), 8.81 (1H, s), 8.16 (1H, d, J = 8.0 Hz), 7.55 (4H, m), 7.35 (4H, m), 5.53 (2H, s), 4.82 (1H, s), 3.58 (2H, d, J = 4.0 Hz), 3.41 (6H, s). Anal. Calcd for $C_{23}H_{22}N_2O_4$: C, 70.75; H, 5.68; N, 7.17. Found: C, 70.94; H, 5.43; N, 7.38.

4.7. Benzyl 1-carbonylmethyl-β-carboline-3-carboxylate (5)

A mixture of 1.09 g (2.79 mmol) of **4**, 10 ml of HOAc, 1.25 ml of HCl and 1.25 ml of water was stirred at room temperature for 4.5 h. To the reaction mixture 100 g of ice was added. The formed precipitates were collected by filtration to provide 642 mg (66.7%) of the title compound, which was used directly in the next step without purification.

4.8. General procedure for preparing *N*-(3-benzyloxycarbonyl-carboline-1-yl)ethylamino acid benzylesters (6a–r)

A mixture of 0.87 mmol of amino acid benzyl esters hydrochloride, 0.24 mmol of NaOH, 10 ml of MeOH and 200 mg (0.58 mmol) of **5** was stirred at room temperature for 10 min, and then 18 mg (0.29 mmol) of $NaBH_3CN$ was added. The reaction mixture was stirred at room temperature for 20 h, adjusted to pH 2 with HCl (3 N) and evaporated under vacuum. The residue was diluted with 20 ml of water, and the aqueous solution was washed with ether (30 ml × 3). The aqueous phase was adjusted to pH 8 with aqueous NaOH (1 N), extracted with EtOAc (100 ml × 3), and the organic phase was separated and washed with saturated aqueous NaCl, and dried over anhydrous sodium sulfate. After filtration the solvent was evaporated under vacuum, and the residue was purified by silica gel chromatography to give **6a–r** in 35–88% yields.

4.8.1. *N*-(3-Benzyloxycarbonylcarboline-1-yl)ethylglycine benzylester (6a)

Yield: 77%. ESI/MS (m/e) 494 $[M+H]^+$; ^{1}H NMR ($CDCl_3$) δ: 10.32 (1H, s), 8.77 (1H, s), 8.15 (1H, d, J = 8.0 Hz), 7.59 (1H, m), 7.43 (1H, d, J = 8.0 Hz), 7.41 (1H, m), 7.39 (2H, m), 7.37 (2H, m), 7.34 (1H, m), 7.33 (2H, m), 7.30 (2H, m), 7.28 (1H, m), 5.52 (2H, s), 5.25 (2H, s), 3.65 (2H, s), 3.47 (2H, t, J = 5.0 Hz), 3.21 (2H, t, J = 5.0 Hz); ^{13}C NMR ($CDCl_3$) δ: 171.58, 166.15, 144.89, 140.92, 136.93, 136.41, 136.15, 135.28, 128.67, 128.57, 128.53, 128.44, 128.35, 128.13, 126.99, 122.03, 121.67, 120.29, 116.91, 112.61, 67.04, 66.92, 50.52, 47.94,

37.05. Anal. Calcd for $C_{30}H_{27}N_3O_4$: C, 73.01; H, 5.51; N, 8.51. Found: C, 72.78; H, 5.38; N, 8.74.

4.8.2. *N*-(3-Benzyloxycarbonylcarboline-1-yl)ethylalanine benzylesters (6b)

Yield: 68%. $[\alpha]_D^{20}$ = 30.49 (*c* 0.01, $CHCl_3$), ESI/MS (m/e) 508 $[M+H]^+$; ^1H NMR ($CDCl_3$) δ: 12.32 (1H, s), 8.72 (1H, s), 8.12 (1H, d, *J* = 7.8 Hz), 7.59 (1H, m), 7.57 (1H, m), 7.42 (1H, m), 7.39 (2H, m), 7.36 (2H, m), 7.33 (3H, m), 7.30 (2H, m), 7.28 (1H, m), 5.49 (2H, s), 4.73 (2H, s), 3.65 (1H, m), 3.37(2H, m), 3.20 (2H, m), 1.50 (3H, s,); ^{13}C NMR ($CDCl_3$) δ: 173.82, 165.94, 143.75, 140.96, 136.66, 136.31, 135.71, 128.66, 128.59, 128.57, 128.53, 128.47, 128.30, 128.24, 127.02, 122.02, 121.68, 120.41, 116.95, 112.47, 67.24, 65.32, 56.24, 52.48, 45.89, 38.05, 17.78. Anal. Calcd for $C_{31}H_{29}N_3O_4$: C, 73.35; H, 5.76; N, 8.28. Found: C, 73.16; H, 5.62; N, 8.07.

4.8.3. *N*-(3-Benzyloxycarbonylcarboline-1-yl)ethylvaline benzylester (6c)

Yield: 68%. $[\alpha]_D^{20}$ = 3.80 (*c* 0.01, $CHCl_3$), ESI/MS (m/e) 536 $[M+H]^+$; ^1H NMR ($CDCl_3$) δ: 12.41 (1H, br s), 8.83 (1H, s), 8.16 (1H, d, *J* = 8.4 Hz), 7.65 (1H, m), 7.62 (1H, m), 7.54 (1H, m), 7.47 (2H, m), 7.42 (2H, m), 7.40 (1H, m), 7.35 (2H, m), 7.30 (2H, m), 7.27 (1H, m), 5.48 (2H, s), 5.17 (2H, s), 3.54 (1H, m), 3.38 (2H, m), 3.12 (2H, m), 2.21 (1H, m), 1.15 (3H, m), 1.12 (3H, m); ^{13}C NMR ($CDCl_3$) δ: 173.90, 166.17, 145.23, 140.68, 136.88, 136.40, 136.22, 135.32, 128.64, 128.55, 128.49, 128.47, 128.38, 128.23, 128.15, 122.19, 121.84, 120.33, 116.94, 112.27, 67.61, 66.95, 66.90, 47.02, 37.59, 31.80, 19.58, 18.95. Anal. Calcd for $C_{33}H_{33}N_3O_4$: C, 74.00; H, 6.21; N, 7.84. Found: C, 74.22; H, 6.36; N, 7.62.

4.8.4. *N*-(3-Benzyloxycarbonylcarboline-1-yl)ethylleucine benzylester (6d)

Yield: 66%. $[\alpha]_D^{20}$ = −3.03 (*c* 0.01, $CHCl_3$), ESI/MS (m/e) 550 $[M+H]^+$; ^1H NMR (DMSO): δ/ppm = 12.38 (1H, br s), 8.61 (1H, s), 8.06 (1H, d, *J* = 8.0 Hz), 7.61 (1H, m), 7.59 (1H, m), 7.52 (1H, m), 7.49 (2H, m), 7.44 (2H, m), 7.41 (1H, m), 7.37 (2H, m), 7.31 (2H, m), 7.16 (1H, m), 5.49 (2H, s), 5.18 (2H, s), 3.68 (1H, m), 3.52 (2H, m), 3.23 (2H, s), 2.01 (1H, m), 1.78 (2H, d, *J* = 5.0 Hz), 1.00 (3H, d, *J* = 5.0 Hz), 0.95 (3H, d, *J* = 5.0 Hz); ^{13}C NMR (DMSO) δ: 171.58, 165.78, 144.04, 140.92, 136.40, 136.34, 135.08, 128.63, 128.60, 128.48, 128.42, 128.37, 127.02, 121.82, 120.41, 116.78, 112.44, 67.23, 66.92, 59.97, 46.36, 41.71, 25.12, 22.65, 22.35. Anal. Calcd for $C_{34}H_{35}N_3O_4$: C, 74.29; H, 6.42; N, 7.64. Found: C, 74.08; H, 6.57; N, 7.41.

4.8.5. *N*-(3-Benzyloxycarbonylcarboline-1-yl)ethylisoleucine benzylester (6e)

Yield: 60%. $[\alpha]_D^{20}$ = 6.57 (*c* 0.01, $CHCl_3$), ESI/MS (m/e) 550 $[M+H]^+$; ^1H NMR ($CDCl_3$) δ: 12.40 (1H, br s), 8.79 (1H, s), 8.17 (1H, d, *J* = 8.4 Hz), 7.62 (1H, m), 7.59 (1H, m), 7.51 (1H, m), 7.49 (2H, m), 7.46 (2H, m), 7.42 (1H, m), 7.32 (2H, m), 7.30 (2H, m), 7.28 (1H, m), 5.52 (2H, s), 5.15 (2H, s), 3.52 (1H, m), 3.47 (2H, m), 3.19 (1H, m), 2.99 (1H, m), 2.07 (1H, m), 1.66 (1H, m), 1.43 (1H, m), 1.08 (3H, d, *J* = 6.9 Hz), 0.97 (3H, t, *J* = 7.5 Hz); ^{13}C NMR ($CHCl_3$) δ: 173.81, 166.19, 145.24, 140.72, 136.91, 136.41, 136.22, 135.35, 128.62, 128.54, 128.48, 128.46, 128.38, 128.22, 128.15, 122.18, 121.48, 120.32, 116.94, 112.23, 66.95, 66.40, 60.41, 47.08, 38.64, 37.56, 25.92, 15.98, 11.71. Anal. Calcd for $C_{34}H_{35}N_3O_4$: C, 74.29; H, 6.42; N, 7.64. Found: C, 74.48; H, 6.58; N, 7.86.

4.8.6. *N*-(3-Benzyloxycarbonylcarboline-1-yl)ethylmethionine benzylester (6f)

Yield: 65%. $[\alpha]_D^{20}$ = −26.55 (*c* 0.01, DMSO), ESI/MS (m/e) 568 $[M+H]^+$; ^1H NMR ($CDCl_3$) δ: 10.94 (1H, s), 8.51 (1H, s), 8.05 (1H, d, *J* = 8.0 Hz), 7.66 (1H, m), 7.64 (1H, m), 7.59 (1H, m), 7.57 (2H, m), 7.48 (2H, m), 7.43 (1H, m), 7.34 (2H, m), 7.31 (m, 2H), 7.20 (1H, m), 5.41 (2H, s), 5.07 (2H, s), 3.50 (1H, m), 3.37 (2H, m), 3.16 (1H, m), 2.99 (1H, m), 2.47 (2H, m), 2.18 (1H, m), 2.08 (1H, m), 2.05 (3H, s); ^{13}C NMR ($CDCl_3$) δ: 166.30, 165.91, 144.61, 140.85, 136.98, 136.68, 136.07, 135.40, 128.76, 128.53, 128.48, 128.43, 128.32, 128.19, 128.09, 121.70, 121.60, 120.52, 116.62, 113.04, 67.17, 67.00, 61.46, 46.46, 36.34, 31.78, 29.73, 29.29. Anal. Calcd for $C_{33}H_{33}N_3O_4S$: C, 69.82; H, 5.86; N, 7.40. Found: C, 69.61; H, 5.71; N, 7.62.

4.8.7. *N*-(3-Benzyloxycarbonylcarboline-1-yl)ethylproline benzylester (6g)

Yield: 68%. $[\alpha]_D^{20}$ = −1.13 (*c* 0.01, DMSO), ESI/MS (m/e) 534 $[M+H]^+$; ^1H NMR ($CDCl_3$) δ: 12.42 (1H, br s), 8.80 (1H, s), 8.17 (1H, d, J = 8.0 Hz), 7.66 (1H, m), 7.64 (1H, m), 7.60 (1H, m), 7.58 (2H, m), 7.56 (2H, m), 7.44 (1H, m), 7.41 (2H, m), 7.38 (2H, m), 7.21 (1H, m), 5.54 (2H, s), 5.11 (2H, s), 3.51 (1H, m), 3.49 (2H, m), 3.30 (2H, m), 2.99 (1H, m), 2.55 (1H, m), 2.30 (1H, m), 2.09 (1H, m), 1.91 (2H, m); ^{13}C NMR ($CDCl_3$) δ: 174.56, 166.26, 145.34, 141.23, 137.04, 136.48, 135.97, 135.16, 128.54, 128.47, 128.36, 128.22, 128.19, 128.14, 127.60, 127.01, 122.04, 121.67, 120.12, 116.93, 112.76, 68.41, 66.98, 66.90, 54.51, 54.12, 36.42, 30.07, 24.00. Anal. Calcd for $C_{33}H_{31}N_3O_4$: C, 74.28; H, 5.86; N, 7.87. Found: C, 74.47; H, 5.70; N, 7.66.

4.8.8. *N*-(3-Benzyloxycarbonylcarboline-1-yl)ethylphenylalanine benzylester (6h)

Yield: 88%. $[\alpha]_D^{20}$ = 10.92 (*c* 0.01, $CHCl_3$); ESI/MS (m/e) 584 $[M+H]^+$; ^1H NMR ($CDCl_3$) δ: 12.42 (1H, br s), 8.79 (1H, s), 8.17 (1H, d, *J* = 8.0 Hz, 7.58 (1H, m), 7.55 (1H, m), 7.48 (1H, m), 7.46 (2H, m), 7.44 (2H, m), 7.42 (1H, m), 7.40 (2H, m), 7.38 (2H, m), 7.35 (2H, m), 7.33 (2H, m), 7.20 (1H, m), 7.15 (1H, m), 5.53 (2H, s), 5.18 (2H, s), 3.80 (1H, m), 3.37 (2H, m), 3.18 (1H, m), 3.13 (1H, m), 3.08 (2H, m); ^{13}C NMR ($CDCl_3$) δ: 173.55, 166.18, 144.99, 140.80, 137.07, 136.89, 136.40, 136.23, 135.55, 135.12, 129.34, 128.85, 128.59, 128.53, 128.47, 128.45, 128.34, 128.16, 127.22, 126.84, 122.05, 121.75, 120.32, 116.93, 112.51, 67.05, 66.95, 62.66, 46.54, 39.16, 37.32. Anal. Calcd for $C_{37}H_{33}N_3O_4$: C, 76.14; H, 5.70; N, 7.20. Found: C, 75.93; H, 5.55; N, 7.01.

4.8.9. *N*-(3-Benzyloxycarbonylcarboline-1-yl)ethyltryptophan benzylester (6i)

Yield: 54%. $[\alpha]_D^{20}$ = 1.13 (*c* 0.01, $CHCl_3$); ESI/MS (m/e) 623 $[M+H]^+$; ^1H NMR (DMSO) δ: 12.20 (1H, s), 10.85 (1H, s), 8.83 (1H, s), 8.39 (1H, d, *J* = 8.0 Hz), 7.63 (1H, m), 7.59 (1H, m), 7.55 (1H, d, *J* = 8.0 Hz), 7.53 (1H, m), 7.51 (1H, m), 7.44 (2H, m), 7.42 (2H, m), 7.40 (1H, m), 7.37 (2H, m), 7.36 (1H, d, *J* = 8.0 Hz), 7.34 (1H, m), 7.24 (1H, s), 7.20 (1H, m), 7.10 (1H, t, *J* = 7.0 Hz), 7.06 (1H, t, *J* = 7.0 Hz), 5.44 (2H, s), 5.02 (2H, s), 3.80 (1H, m), 3.40 (1H, m), 3.34 (2H, m), 3.01 (1H, m), 2.90 (2H, m); ^{13}C NMR ($CDCl_3$) δ: 175.46, 165.96, 145.00, 141.27, 136.63, 136.61, 136.51, 136.48, 136.30, 128.65, 128.57, 128.50, 128.45, 128.39, 128.25, 128.16, 127.86, 124.17, 127.02, 122.62, 121.80, 121.32, 120.60, 118.69, 116.74, 112.82, 111.80, 110.24, 66.37, 65.98, 62.79, 60.50, 46.77, 31.22, 29.34. Anal. Calcd for $C_{39}H_{35}N_3O_6$: C, 72.99; H, 5.50; N, 6.55. Found: C, 72.78; H, 5.67; N, 6.78.

4.8.10. *N*-(3-Benzyloxycarbonylcarboline-1-yl)ethylserine benzylester (6j)

Yield: 68%. $[\alpha]_D^{20}$ = −7.89 (*c* 0.01, $CHCl_3$); ESI/MS (m/e) 524 $[M+H]^+$; ^1H NMR (DMSO) δ: 12.29 (1H, s), 8.81 (1H, s), 8.37 (1H, d, *J* = 8.30 Hz), 7.67 (1H, m), 7.64 (1H, m), 7.61 (1H, m), 7.59 (2H, m), 7.56 (2H, m), 7.53 (1H, m), 7.44 (2H, m), 7.31 (2H, m), 7.24 (1H, m), 5.42 (2H, s), 5.11 (2H, s), 3.92 (1H, m), 3.72 (1H, m), 3.57 (1H, m), 3.15 (2H, m), 2.97 (2H, m). ^{13}C NMR (DMSO) δ: 173.42, 165.93, 145.04, 141.21, 137.05, 136.59, 136.31, 128.95,

128.78, 128.51, 128.32, 128.15, 127.60, 122.59, 121.77, 120.58, 116.75, 112.87, 66.35, 65.98, 63.55, 62.79, 46.63, 34.88. Anal. Calcd for $C_{31}H_{29}N_3O_5$: C, 71.11; H, 5.58; N, 8.03. Found: C, 71.30; H, 5.42; N, 7.81.

4.8.11. *N*-(3-Benzyloxycarbonylcarboline-1-yl)ethylthreonine benzylester (6k)

Yield: 62%. $[\alpha]_D^{20} = -11.02$ (*c* 0.01, $CHCl_3$); ESI/MS (m/e) 538 $[M+H]^+$; ^1H NMR ($CDCl_3$) δ: 12.34 (1H, s), 8.73 (1H, s), 8.13 (1H, d, *J* = 8.0 Hz), 7.59 (1H, t, *J* = 8.0 Hz), 7.55 (1H, m), 7.52 (1H, m), 7.41 (2H, m), 7.39 (2H, m), 7.37 (1H, m), 7.34 (2H, m), 7.31 (m, 2H), 7.28 (2H, m), 5.48 (2H, s), 5.17 (2H, s), 4.06 (1H, m), 3.69 (1H, m), 3.32 (2H, m), 3.25 (2H, m), 1.31 (3H, d, *J* = 4.0 Hz); ^{13}C NMR ($CDCl_3$) δ: 172.68, 166.85, 144.06, 140.86, 136.56, 136.26, 136.16, 135.00, 128.64, 128.64, 128.52, 128.46, 128.29, 128.21, 121.95, 121.69, 120.49, 116.83, 112.47, 68.31, 68.21, 67.26, 52.62, 46.85, 35.95, 21.79. Anal. Calcd for $C_{32}H_{31}N_3O_5$: C, 71.49; H, 5.81; N, 7.82. Found: C, 71.28; H, 5.97; N, 7.60.

4.8.12. *N*-(3-Benzyloxycarbonylcarboline-1-yl)ethylasparagine benzylester (6l)

Yield: 33%. $[\alpha]_D^{20} = -31.14$ (*c* 0.01, $CHCl_3$); ESI/MS (m/e) 551 $[M+H]^+$; ^1H NMR ($CDCl_3$) δ: 11.19 (1H, s), 8.84 (1H, s), 8.38 (1H, d, *J* = 8.0 Hz), 7.68 (1H, d, *J* = 8.0 Hz), 7.60 (1H, t, *J* = 8.0 Hz), 7.58 (1H, m), 7.54 (2H, m), 7.52 (2H, m), 7.44 (2H, m), 7.40 (2H, m), 7.30 (2H, m), 7.24 (1H, m), 5.42 (2H, s), 5.07 (2H, s), 3.71 (1H, m), 3.31 (2H, m), 3.29 (1H, m), 3.09 (1H, m), 2.74 (2H, m); ^{13}C NMR ($CDCl_3$) δ: 177.62, 173.99, 165.94, 144.96, 141.23, 137.05, 136.57, 136.36, 128.97, 128.88, 128.75, 128.55, 12.47, 128.30, 128.18, 127.62, 122.59, 121.78, 120.60, 116.75, 112.92, 66.37, 66.05, 58.07, 46.06, 37.50, 34.69. Anal. Calcd for $C_{32}H_{30}N_4O_5$: C, 69.80; H, 5.49; N, 10.18. Found: C, 69.61; H, 5.33; N, 10.39.

4.8.13. *N*-(3-Benzyloxycarbonylcarboline-1-yl)ethylglutamine benzylester (6m)

Yield: 68%. $[\alpha]_D^{20} = -5.8$ (*c* 0.01, $CHCl_3$); ESI/MS (m/e) 565 $[M+H]^+$; ^1H NMR ($CDCl_3$) δ: 12.12 (1H, s), 8.86 (1H, s), 8.24 (1H, d, *J* = 8.0 Hz), 7.61 (1H, m), 7.59 (1H, m), 7.57 (1H, m), 7.54 (2H, m), 7.51 (2H, m), 7.43 (1H, m), 7.41 (1H, m), 7.32 (2H, m), 7.26 (1H, m), 5.42 (2H, s), 5.07 (2H, s), 3.65 (1H, m), 3.36 (2H, m), 3.12 (1H, m), 2.97 (1H, m), 2.22 (2H, m), 2.07 (2H, m); ^{13}C NMR ($CDCl_3$) δ: 175.16, 173.69, 166.47, 143.47, 142.44, 137.22, 137.07, 136.82, 128.70, 128.54, 128.53, 128.45, 128.27, 128.21, 121.67, 121.59, 120.58, 116.30, 110.34, 68.20, 67.32, 67.25, 47.40, 37.68, 34.4527.42. Anal. Calcd for $C_{33}H_{32}N_4O_5$: C, 70.20; H, 5.71; N, 9.92. Found: C, 70.01; H, 5.56; N, 9.70.

4.8.14. *N*-(3-Benzyloxycarbonylcarboline-1-yl)ethyltyrocine benzylester (6n)

Yield: 69%. $[\alpha]_D^{20} = 8.83$ (*c* 0.01, $CHCl_3$); ESI/MS (m/e) 600 $[M+H]^+$; ^1H NMR ($CDCl_3$) δ: 12.43 (1H, s), 8.78 (1H, s), 8.14 (1H, d, *J* = 8.0 Hz), 7.56 (1H, m), 7.52 (1H, m), 7.50 (1H, m), 7.40 (2H, m), 7.38 (2H, m), 7.36 (1H, m), 7.32 (2H, m), 7.28 (2H, m), 7.22 (1H, m), 6.92(2H, m), 6.67(2H, m), 5.47 (2H, s), 5.18 (2H, s), 3.78 (1H, m), 3.32 (1H, m), 3.23 (1H, m), 3.07 (2H, m), 2.98 (2H, m); ^{13}C NMR ($CDCl_3$) δ: 173.65, 166.09, 155.66, 144.69, 140.93, 136.85, 136.18, 135.39, 135.09, 130.95, 130.22, 130.03, 128.65, 128.61, 128.55, 128.52, 128.42, 128.22, 127.83, 126.92, 121.90, 121.76, 120.43, 117.02, 115.99, 115.80, 112.58, 67.12, 66.99, 62.79, 46.46, 39.67, 36.30. Anal. Calcd for $C_{37}H_{33}N_3O_5$: C, 74.11; H, 5.55; N, 7.01. Found: C, 74.30; H, 5.40; N, 6.79.

4.8.15. *N*-(3-Benzyloxycarbonylcarboline-1-yl)ethylaspartic acid dibenzylester (6o)

Yield: 50%. $[\alpha]_D^{20} = -7.96$ (*c* 0.01, $CHCl_3$); ESI/MS (m/e) 642 $[M+H]^+$; ^1H NMR ($CDCl_3$): δ/ppm = 12.11 (1H, s), 8.82 (1H, s), 8.37 (1H, d, *J* = 8.0 Hz), 7.67 (1H, m), 7.61 (1H, m), 7.59 (1H, m), 7.56 (m, 2H), 7.52 (2H, m), 7.49 (1H, m), 7.41 (5H, m), 7.38 (4H, m), 7.22 (1H, m), 5.40 (2H, s), 5.04 (s, 2H), 4.98 (2H, s), 3.75 (1H, m), 3.28 (1H, m), 3.23 (2H, m), 3.10 (1H, m), 2.74 (2H, m); ^{13}C NMR ($CDCl_3$) δ: 173.24, 170.78, 165.94, 144.87, 141.23, 137.04, 136.57, 136.45, 136.37, 136.32, 128.92, 128.85, 128.81, 128.74, 128.63, 128.45, 128.38, 128.30, 128.24, 127.62, 127.06, 126.87, 122.57, 121.80, 120.59, 116.67, 112.82, 66.34, 66.30, 66.05, 57.80, 46.42, 37.77, 34.47. Anal. Calcd for $C_{39}H_{35}N_3O_6$: C, 72.99; H, 5.50; N, 6.55. Found: C, 72.78; H, 5.36; N, 6.33.

4.8.16. N^{α}-(3-Benzyloxycarbonylcarboline-1-yl)-N^{ω}-(benzyloxycarbonyl)ethyllysine benzylester (6p)

Yield: 54%. $[\alpha]_D^{20} = 2.53$ (*c* 0.01, $CHCl_3$); ESI/MS (m/e) 699 $[M+H]^+$; ^1H NMR (DMSO) δ: 12.10 (1H, br s), 8.76 (1H, s), 8.14 (1H, d, *J* = 8.0 Hz), 7.54 (1H, m), 7.44 (1H, m), 7.40–7.42 (6H, m), 7.35–7.37 (5H, m), 7.32–7.34 (6H, m), 5.24 (2H, s), 5.16 (2H, s), 5.07 (2H, s), 3.74 (1H, m), 3.43 (2H, m), 3.18 (2H, m), 3.08 (2H, m), 1.77 (2H, m), 1.50 (2H, m), 1.35 (2H, m). ^{13}C NMR (DMSO) δ: 175.82, 166.13, 156.39, 145.00, 140.75, 136.86, 136.62, 136.51, 136.39, 135.70, 135.34, 128.63, 128.52, 128.36, 128.12, 122.10, 121.84, 120.38, 116.90, 112.25, 66.95, 66.68, 65.86, 61.40, 46.60, 40.82, 34.36, 29.67, 22.76. Anal. Calcd for $C_{42}H_{42}N_4O_6$: C, 72.19; H, 6.06; N, 8.02. Found: C, 72.00; H, 6.22; N, 8.26.

4.8.17. *N*-(3-Benzyloxycarbonylcarboline-1-yl)ethylhistidine benzylester (6q)

Yield: 42%. $[\alpha]_D^{20} = -7.99$ (*c* 0.01, $CHCl_3$); ESI/MS (m/e) 574 $[M+H]^+$; ^1H NMR (DMSO) δ: 12.82 (1H, br s), 12.45 (1H, br), 8.87 (1H, s), 8.67 (1H, m), 8.40 (1H, d, *J* = 8.0 Hz), 7.69 (1H, m), 7.61 (1H, m), 7.43 (1H, m), 7.39 (4H, m), 7.35 (4H, m), 7.24 (2H, m), 5.42 (2H, s), 4.49 (2H, s), 3.65 (1H, m), 3.28 (1H, m), 3.23 (2H, m), 3.10 (1H, m), 2.78 (2H, m).;^{13}C NMR (DMSO) δ: 172.51, 166.47, 143.00, 140.96, 136.67, 136.33, 135.70, 133.50, 128.65, 128.58, 128.56, 128.53, 128.47, 128.31, 128.24, 127.04, 122.01, 121.69, 120.41, 119.42, 116.95, 112.47, 63.34, 63.27, 59.90, 45.59, 37.77, 34.87. Anal. Calcd for $C_{34}H_{31}N_5O_4$: C, 71.19; H, 5.45; N, 12.21. Found: C, 70.99; H, 5.30; N, 12.00.

4.8.18. *N*-(3-Benzyloxycarbonylcarboline-1-yl)ethylglutamic acid dibenzylester (6r)

Yield: 57%. $[\alpha]_D^{20} = -30.05$ (*c* 0.01, DMSO), ESI/MS (m/e) 548 $[M+H]^+$; ^1H NMR ($CDCl_3$) δ: 11.22 (1H, s), 8.78 (1H, s), 8.17 (1H, d, *J* = 8.4 Hz), 7.67 (1H, m), 7.64 (1H, m), 7.60 (1H, m), 7.56 (2H, m), 7.53 (2H, m), 7.43 (1H, m), 7.40 (2H, m), 7.37 (2H, m), 7.28 (1H, m), 5.54 (2H, s), 5.11 (2H, s), 3.51 (1H, m), 3.30 (2H, m), 2.99 (2H, m), 2.55 (1H, m), 2.30 (1H, m), 2.22 (1H, m), 2.09 (1H, m). ^{13}C NMR ($CDCl_3$) δ: 174.56, 166.26, 145.34, 141.23, 137.04, 136.48, 135.97, 135.16, 128.54, 128.47, 128.36, 128.22, 128.19, 128.14, 127.60, 127.01, 122.04, 121.67, 120.12, 116.93, 112.76, 68.41, 66.98, 66.90, 54.51, 54.12, 36.42, 30.07, 24.00. 177.75, 171.70, 166.04, 142.79, 140.97, 136.63, 135.07, 134.94, 128.77, 128.72, 128.67, 128.62, 128.57, 128.47, 128.40, 128.20, 127.58, 127.00, 121.89, 120.56, 117.30, 112.51, 67.56, 66.96, 61.56, 41.99, 33.67, 29.64, 24.80. Anal. Calcd for $C_{33}H_{29}N_3O_5$: C, 72.38; H, 5.34; N, 7.67. Found: C, 72.16; H, 5.18; N, 7.44.

4.9. Bioassay

4.9.1. In vitro anti-proliferation assay of 6a–r

According to the slightly modified procedure of Al-Allaf and Rashan,[9] the in vitro anti-proliferation assays were carried out by use of 96 microtiter plate cultures and MTT staining. The $HepG_2$, Hela, Bel7402, K562, and B16 cells (final concentration in the growth medium was 1×10^4/ml) were grown in RPMI-1640 medium (containing 10%, v/v) FCS, penicillin (100 μg/ml) and streptomycin

(100 μg/ml) without (for control) or with **6a–r** (in a series of final concentrations ranging from 0.1 μM to 200 μM). The cultures were propagated at 37 °C in a humidified atmosphere containing 5% CO_2 for 24 h, after the first renew of the growth medium without (for control) or with **6a–r** (for test sample) were propagated for another 48 h, after the second renew of the growth medium with 25 μl of MTT solution (5 mg/ml) were propagated for another 4 h. The growth medium was removed and the residue was dried in the air. The dried residues were dissolved in 100 μl of DMSO and the absorption values of light of the formed purple solutions were recorded on Bio-rad 570 microplate reader (Biorad, USA). The inhibited rates were calculated according to $I\% = \%\ (C - T/C)$. Wherein C presents the absorption value of light of the control and T presents the absorption value of light of the test sample. The IC_{50} values were determined via program GWBASIC.EXE.

4.9.2. In vivo anti-tumor assay of 6a–r

Male ICR mice, purchased from Peking University Health Science Center, were maintained at 21 °C with a natural day/night cycle in a conventional animal colony. The mice were 10–12 weeks old at the beginning of the experiments. The tumor used was S180 that forms solid tumors, when injected subcutaneously. S180 cells for initiation of subcutaneous tumors were obtained from the ascitic form of the tumors in mice, which were serially transplanted once per week. Subcutaneous tumors were implanted by injecting 0.2 ml of NS containing 1×10^7 viable tumor cells under the skin on the right oxter. Twenty-four hours after implantation, the tumor-bearing mice were randomized into 20 experimental groups (10 per group). All the mice were given a daily ip injection of cytarabine (positive control, 8.9 μmol/kg/day in 0.2 ml of NS), or NS (negative control, 0.2 ml), or **6a–r** (8.9 μmol/kg/day in 0.2 ml of NS) for seven consecutive days. Twenty-four hours after the last administration, all mice were sacrificed by diethyl ether anesthesia and the tumor wet weights of the treated (T_w) and control (C_w) groups were measured on the last day of each experiment and the percentage of tumor growth inhibition was calculated as follows:

$$\text{Inhibition } (\%) = [1 - (T_w/Cw)] \times 100$$

4.9.3. In vivo dose-dependent assay of oral administration of 6j,o

Male ICR mice, purchased from Peking University Health Science Center, were maintained at 21 °C with a natural day/night cycle in a conventional animal colony. The mice were 10–12 weeks old at the beginning of the experiments. The tumor used was S180 that forms solid tumors, when injected subcutaneously. S180 cells for initiation of subcutaneous tumors were obtained from the ascitic form of the tumors in mice, which were serially transplanted once per week. Subcutaneous tumors were implanted by injecting 0.2 ml of NS containing 1×10^7 viable tumor cells under the skin on the right oxter. Twenty-four hours after implantation, the tumor-bearing mice were randomized into 20 experimental groups (10 per group). All the mice were given a daily ip injection of cytarabine (positive control, 89, 8.9 or 0.9 μmol/kg/day in 0.2 ml of NS), or a daily oral administration of NS (negative control, 0.2 ml), or **6j,o** (89, 8.9 or 0.9 μmol/kg/day in 0.2 ml of NS) for seven consecutive days. Twenty-four hours after the last administration, all mice were sacrificed by diethyl ether anesthesia and the tumors were dissected and weighed. The inhibitory rate of tumor growth was calculated according to the formula of Section 4.9.2.

4.10. Viscometric measurement

Ostwald type viscometer, immersed in a thermostated water bath maintained at 28 °C, was used. CT DNA or **6d** was dissolved in phosphate buffer to prepare solutions. Sample solutions were prepared by adding **6d** solution separately to DNA solution so as to give the [**6d**]/[DNA] ratios in the range of 0–0.36. The flow time of the sample solutions were measured after a thermal equilibrium time of 5 min. The flow time of each sample was calculated. The relative viscosity of DNA in the presence and absence of **6d** were calculated according $\eta = (t - t_0)/t_0$, where t_0 and t were the observed flow time in the absence and presence of **6d**. Data has been presented as $(\eta/\eta_0)^{1/3}$ versus binding ratio, where η is the viscosity of DNA in the presence of **6d** and η_0 is the viscosity of DNA alone.

Acknowledgments

This work was completed in the Beijing area major laboratory of peptide and small molecular drugs, supported by PHR (IHLB, KM 200910025010), the National Natural Scientific Foundation of China (30901843, 30801426), and Special Project (2008ZX09401-002) of China.

References and notes

1. Momekov, G.; Bakalova, A.; Karavanova, M. *Curr. Med. Chem.* **2005**, *12*, 2177.
2. Bolognese, A.; Correale, G.; Manfra, M.; Lavecchia, A.; Mazzoni, O.; Novellino, E.; La Colla, P.; Sanna, G.; Loddo, R. *J. Med. Chem.* **2004**, *47*, 849.
3. Lynch, M. A.; Duval, O.; Sukhanova, A.; Devy, J.; Mackay, S. P.; Waigh, R. D.; Nabiev, I. *Bioorg. Med. Chem. Lett.* **2001**, *11*, 2643.
4. Cao, R.; Peng, W.; Chen, H.; Ma, Y.; Liu, X.; Hou, X.; Guan, H.; Xu, A. *Biochem. Biophys. Res. Commun.* **2005**, *338*, 1557.
5. Laronze, M.; Boisbrun, M.; Leonce, S.; Pfeiffer, B.; Renard, P.; Lozach, O.; Meijer, L.; Lansiaux, A.; Bailly, C.; Sapi, J.; Laronze, J. Y. *Bioorg. Med. Chem.* **2005**, *13*, 2263.
6. Sobhani, A. M.; Ebrahimi, S. A.; Mahmoudian, M. *J. Pharm. Pharm. Sci.* **2002**, *5*, 19.
7. Zhao, M.; Bi, L.; Wang, W.; Wang, C.; Baudy-Floc, M.; Ju, J.; Peng, S. *Bioorg. Med. Chem.* **2006**, *14*, 6998.
8. Wu, J. H.; Zhao, M.; Qian, K. D.; Lee, K. H.; Natschke, S. M.; Peng, S. Q. *Eur. J. Med. Chem.* **2009**, *44*, 4153.
9. Sobhani, A. M.; Amini, S. R.; Tyndall, J. D. A.; Azizi, E.; Daneshtalab, M.; Khalaj, A. *J. Mol. Graphics Modell.* **2006**, *25*, 459.
10. Marco, A.; Loza-Mejía; Rafael, C.; Alfonso, L. R. *J. Mol. Graphics Modell.* **2009**, *27*, 900.
11. Alves, C. M. A.; Naik, S.; Coutinho, P. J. G. *Tetrahedron* **2009**, *65*, 10441.
12. Venkatachalam, C. M.; Jiang, X.; Oldfield, T.; Waldman, M. *J. Mol. Graphics Modell.* **2003**, *21*, 289.
13. Rezaei, Z.; Firouzabadi, H.; Iranpoor, N.; Ghaderi, A.; Jafari, M. R.; Jafari, A. A.; Zare, H. R. *Eur. J. Med. Chem.* **2009**, *44*, 4266.
14. Li, N.; Ma, Y.; Yang, C.; Guo, L. P.; Yang, X. R. *Biophys. Chem.* **2005**, *116*, 199.
15. Queiroz, R. P.; Castanheir, M. S. E.; Lopes, C. T. T.; Cruz, K. Y.; Kirsch, G. *J. Photochem. Photobiol., A.* **2007**, *190*, 45.
16. Varadarajan, U.; Alfonso, C.; Balachandran, U. N. *Polyhedron* **2007**, *26*, 3008.
17. Maheswari, P. U.; Palaniandavar, M. *J. Inorg. Biochem.* **2004**, *98*, 219.
18. Pitchumony, T. S.; Evans, H. S.; Palaniandavar, M. *J. Inorg. Biochem.* **2005**, *99*, 2110.
19. Arjmand, F.; Aziz, M. *Eur. J. Med. Chem.* **2009**, *44*, 834.
20. Shi, S.; Xie, T.; Yao, T. M.; Wang, C. R.; Geng, X. T.; Yang, D. J.; Han, L. J.; Ji, L. N. *Polyhedron* **2009**, *28*, 1355.
21. Hsin, L. W.; Wang, H. P.; Kao, P. H.; Lee, O.; Chen, W. R.; Chen, H. W.; Guh, J. H.; Chan, Y. L.; His, C. P.; Yang, M. S.; Li, T. K.; Lee, C. H. *Bioorg. Med. Chem.* **2008**, *16*, 1006.
22. MacKerell, A., Jr.; Banavali, N. *J. Comput. Chem.* **2000**, *21*, 105.
23. Shaikh, A. R.; Ismael, M.; Carpio, C. A. D.; Tsuboi, H.; Koyama, M.; Endou, A.; Kubo, M.; Broclawikc, E.; Miyamoto, A. *Bioorg. Med. Chem. Lett.* **2006**, *16*, 5917.
24. Doddareddy, M. R.; Cho, Y. S.; Koh, H. Y.; Pae, A. N. *Bioorg. Med. Chem.* **2004**, *12*, 3977.